Vol 5 (1) (2024)

Measurement, Control, and Automation

Website: https:// mca-journal.org

ISSN 1859-0551

# Stability analysis of *I-f* startup method for PMSM drive systems

**Truong Nguyen Van[1], Xuan Cuong Cao[1], Van Vuong Dinh[2], Anh Tan Nguyen[1,*]**

[1]*School of Electrical and Electronic Engineering, Hanoi University of Science and Technology, Hanoi, 10000, Vietnam*
[2]*Faculty of Electrical and Electronic Engineering, Hanoi College of High Technology, Hanoi, 10000, Vietnam*
[*]*Corresponding author E-mail: tan.nguyenanh@hust.edu.vn*

## Abstract

In low-cost permanent magnet synchronous motor (PMSM) drive systems, the rotor position is usually estimated based on the back-electromotive force. However, such estimation methods have the common drawback of having large errors in low-speed regions. In order to solve that drawback in the startup phase, the *I-f* startup method is studied as its compatibility with the FOC control structure. The purpose of such a method is to make the motor accelerate and overcome the low-speed threshold. The process of implementing the *I-f* startup algorithm is divided into two stages, the first one is acceleration stage, and the second one is smooth transition stage. During the acceleration phase, the motor speed is controlled using a constant-magnitude current vector located on a virtual rotating reference frame. Analyzes of possible oscillations and causes of system instability during the startup phase are clarified in this study. The requirement of the parameters of the virtual rotating reference frame and the current vector for ensuring the acceleration process is under control is presented. The smooth transition stage is added so that large peak current pulses do not occur when switching from startup mode to closed-loop control mode. The algorithm for reducing the virtual current vector magnitude by a simple linear ramp function is shown in this paper. The analysis is verified through the simulation results.

***Keywords***: *Acceleration; Electrical angle error; FOC; I-f startup; PMSM; Self-stabilizing; Sensorless control; Smooth transition; Virtual rotating reference frame*

## Symbol

| Symbol | Unit | Describe |
|---|---|---|
| $u_d$, $u_q$ | V | *d-q* axis voltages |
| $i_d$, $i_q$ | A | *d-q* axis currents |
| $i_d^*$, $i_q^*$ | A | *d-q* axis reference currents |
| $i_{qs}^*$ | A | *q* axis startup current |
| $R_s$ | Ω | Stator phase resistance |
| $L_s$ | H | Stator phase inductance |
| $L_d$, $L_q$ | H | *d-q* axis inductance |
| $\lambda_m$ | Wb | Rotor flux |
| $\omega_e$, $\omega_r$ | rad/s | Electromagnetic and mechanical angular speeds |
| $\omega_{es}^*$ | rad/s | Virtual reference angular speed |
| $p$ | | Pole pairs |
| $\theta_e$ | rad | Rotor electrical angle |
| $\theta_{e0}$ | rad | Initial electrical angle |
| $\theta_{es}^*$ | rad | Virtual electrical angle |
| $\Delta\theta_e$ | rad | Electric angle error |
| $\gamma_{es}^*$ | rad/s$^2$ | Virtual angular acceleration |
| $\delta_\gamma$ | % | Relative angular error |
| $T_e$ | Nm | Electromagnetic moment |
| $T_L$ | Nm | Load moment |
| $T_{L0}$ | Nm | Initial load moment |
| $k_L$ | | Squared scaling factor |
| $J_m$ | kgm$^2$ | Inertia moment |

## Nomenclature

| | |
|---|---|
| PMSM | Permanent magnet synchronous motors |
| SPMSM | Surface-mounted PMSM |
| FOC | Field oriented control |
| HFSI | High frequency signal injection |
| PI | Proportional integral |
| B-EMF | Back-electromotive force |

## 1. Introduction

PMSM is gradually gaining popularity recently dues to the compactness, high performance and low noise suitable for industrial and electric vehicle applications. Field-Oriented Control (FOC) is the classic control method for PMSM drive systems [1]. The FOC algorithm requires converting the stator current components from a stationary reference frame to rotating reference frame using the Park transform. The implementation of FOC algorithm requires real-time feedback of stator current and rotor position.

In some low-cost applications, rotor position estimation algorithms are based on back-electromotive force (B-EMF) [2],[3] are used instead of using actual measuring devices. However, this method has large errors at low-speed regions negatively affecting the FOC algorithm. A method to improve rotor position estimation at low speeds or to increase the motor speed to a threshold high enough for FOC to be performed accurately is necessary.

Received: 17 January 2024; Accepted: 18 March 2024.

A method to improve rotor position estimation for PMSM can be mentioned as high frequency signal injection (HFSI) [4], [5], [6], which can determine the rotor position over the motor speed ranges. The HFSI is performed based on the estimation of the minimum inductance position using a loop of measuared current differential calculations combined with filters. However, the complex algorithm also introduces high-order harmonic components in the curent, so this method is not necessary for low-cost applications such as pumps, fans or compressors.

A startup method allow accelecrate the motor through low speed is *V/f*, be widely used in asynchronous AC motor control, has been researched for use in PMSM drive systems [7], [8]. The *V/f* method has an open structure with no current or position feedback, and it is simple for implementation. However, using the *V/f* structure to start the PMSM faces many difficulties when switching to FOC since one structure is scalar control and the orther is vector control.

Since 1990, *I-f* startup method was proposed [9]. Due to the increasing demand for PMSM, there has been much research over the past decade about the *I-f* startup method [10-17]. This method has a structue that the FOC current closed-loop combined with speed open-loop control. Most of these research show that *I-f* has two stages, the first stage accelerates the motor beyond the low speed threshold and the next stage is smooth transition, convert from the open-loop to closed control.

In the acceleration stage, the motor is accelerated by establishing a large enough current vector on the virtual rotating reference frame and injecting to the FOC current controller. The binding condition between the magnitude of the current vector and the rotation speed of the virtual rotating reference frame has been shown in [11-15] but optimal selections of parameters has not been presented. Study in [13] has shown that oscillations can be occurred if acceleration of the virtual rotating frame are too small, but analyses for various load conditions and applications have not shown. Another thing that needs to be mentioned is the angle error between the virtual rotating reference frame and the real rotating reference frame (rotating frame associated with the rotor flux vector) at the starting time also affects the stability of system. Although these reseachs [12], [13], [17] showed the conditon about the first angle error, it was not detailed, clear and not entirely true for light or heavy starting load conditions.

Since the virual current vector which is injected into the FOC current controller is much larger to generate an electromagnetic torque that is balanced with the load torque, leading to the existence of the rotating frame angle errors after the end of the accelaration stage. If the system immediately switch the speed controller from open-loop to closed-lopp mode, it will cause very large torque and current pulses, adversely affecting the mechanical and electrical systems. Due to that, a smooth transition phase must be performed to reduce the angle error between the two rotating reference frames before switching control modes. Studies [10], [12], [15] proposed nonlinear current reduction algorithm based on the Euler exponential function, while studies [11], [14], [17] use the algorithm for linearly reducing the reference current based on the slope function.

Although the *I-f* method has been shown and there was much research, it has not been analyzed enough. The contribution of this paper is to analyze the stability conditions for the PMSM drive system when performing acceleration and smooth shifting with the *I-f* startup method. Fluctuations may occur when inappropriate acceleration parameters are selected or/and the presence in angle difference between the virtual rotating reference frame and the real rotating reference frame during acceleration phase. The method of reducing the amount of current using the slope function is used to make the algorithm simpler in the smooth transition stage. PMSMs are classified into two types [18] but this paper is mainly aimed at surface-mounted permanent magnet synchronous motors (SPMSM). To verify the *I-f* starting method by simulation and evaluate the applicability for some practical applications, a load which has mechanical characteristics like an industrial fan is considered.

In this paper, the mathematical model and control structure for SPMSM are presented in section 2, the analysis of the theoretical basis of the *I-f* algorithm is stated in section 3, the simulation results and discussion are shown in section 4, and the conclusions are stated in section 5.

## 2. Control configuration of SPMSM drives

### 2.1. SPMSM modeling

The modeling of SPMSM can be expressed in synchronous rotating *dq* reference frame:

$$u_d = R_s i_d + L_s \frac{di_d}{dt} - \omega_e L_s i_q \tag{1}$$

$$u_q = R_s i_q + L_s \frac{di_q}{dt} + \omega_e L_s i_d + \omega_e \lambda_m \tag{2}$$

Since SPMSM has equal axial inductance components $L_d$ and transverse inductance $L_q$ [18], in equations (1) and (2) only use the symbol $L_s$ to replace $L_d$ and $L_q$.

The relationship between the electrical angular speed and the rotor mechanical angular speed is determined as follows:

$$\omega_e = p\omega_r \tag{3}$$

The rotor electrical angle is determined according to the electrical angular speed as follows:

$$\theta_e = \int \omega_e dt + \theta_{e0} \tag{4}$$

The electromagnetic torque of SPMSM is determined according to the following expression:

$$T_e = \frac{3}{2} p\lambda_m i_q \tag{5}$$

The kinetic equation of SPMSM is determined according to the following expression:

$$\frac{d\omega_r}{dt} = \frac{T_e - T_L}{J_m} \tag{6}$$

### 2.2. SPMSM drive control configuration

The overview structure of the SPMSM drive control system is shown in Figure 1, including an FOC-type closed current

loop, an *I-f* startup open loop, and a speed control closed loop. The *I-f* startup open-loop and the speed control closed-loop cannot be executed at the same time, so a switch between two consecutive processes (pin 1 and pin 2) is added. Pin 1 is connected to the values set from the algorithm of the *I-f* startup process, pin 2 is connected to the output of the speed controller. All these pins conduct signals to the internal FOC current loop.

The current loop plays a role in controlling the electromagnetic process in the motor stator. The current controller implements an algorithm to control a current vector consisting of two components, the *d*-axis current $i_d$ and the *q*-axis current $i_q$ components. Two PI linear control channels combined with interchannel noise compensation are used [1]. To compensate for disturbances caused by B-EMF, the value of the rotor electric angular speed needs to be determined and put into the current controller. From (5) function, the electromagnetic torque produced is linearly proportional to $i_q$ and does not depend on $i_d$. Therefore, $i_d^*$ is set to zero to achieve maximum torque per ampere control as well as reduce power loss. The current $i_q^*$ is the output of the speed controller. To perform the transition from a stationary reference frame to a rotating reference frame or vice versa, the rotor electric angle value needs to be determined.

The role of the speed control loop is to regulate the mechanical process on the motor rotor. Two control processes are performed consecutively in this loop. To be concise in naming the control algorithm implementation processes, the *I-f* startup algorithm implementation process is called *I-f mode*, and the traditional PI algorithm implementation process is called *PI mode*. *PI mode* is based on the error between the reference speed and feedback speed to calculate the amount of $i_q^*$ which generate electromagnetic torque so it can be considered as a closed loop control. *I-f mode* does not need speed or position feedback values but is based on pre-determined system parameters and conditions, so it is considered an open loop circuit. *I-f mode* is divided into two stages, the first stage is acceleration, and the second stage is smooth transition stage. The theoretical analysis of the *I-f mode*, as well as the two stages of algorithm implementation, are presented in detail in section 3.

## 3. *I-f* startup method

### 3.1. Acceleration stage

The purpose of the acceleration stage is bringing the motor rotor past a low speed threhold, typically around 15% to 35% of rated speed.

From function (3), (5) and (6) can be rewriten as follows:

$$\frac{1}{p}\frac{d\omega_e}{dt} = \frac{1.5p\lambda_m i_q - T_L}{J_m} \tag{7}$$

According to (7), the rotor can accelerate by applying a sufficiently large current $i_q^*$. Therefore, the FOC algorithm requires precise angular position of the rotor flux vector, which is not available at low speeds. Instead, the *I-f* starting method uses a virtual current vector associated with a virtual rotating reference frame, with following parameters: $i_{qs}^*$ is the virtual reference current vector magnitude, $\gamma_{es}^*$ is the angular acceleration of the virtual rotating reference frame, $\omega_{es}^*$ is angular speed of virtual rotating reference frame, $\theta_{es}^*$ is angular position of the virtual rotating reference frame relative to the real reference frame. The two parameters $i_{qs}^*$ and $\gamma_{es}^*$ have constant positive values during the acceleration stage. The angular speed and angular position of the virtual rotating reference frame are expressed over time as follows:

$$\omega_{es}^* = \gamma_{es}^* t \tag{8}$$

$$\theta_{es}^* = \frac{1}{2}\gamma_{es}^* t^2 + \theta_{es0}^* \tag{9}$$

Since there is no position feedback and the magnitude of the electromagnetic torque can be changed, the electrical angle difference between the real rotating reference frame and the virtual rotating reference frame can exist. That difference is defined as follows:

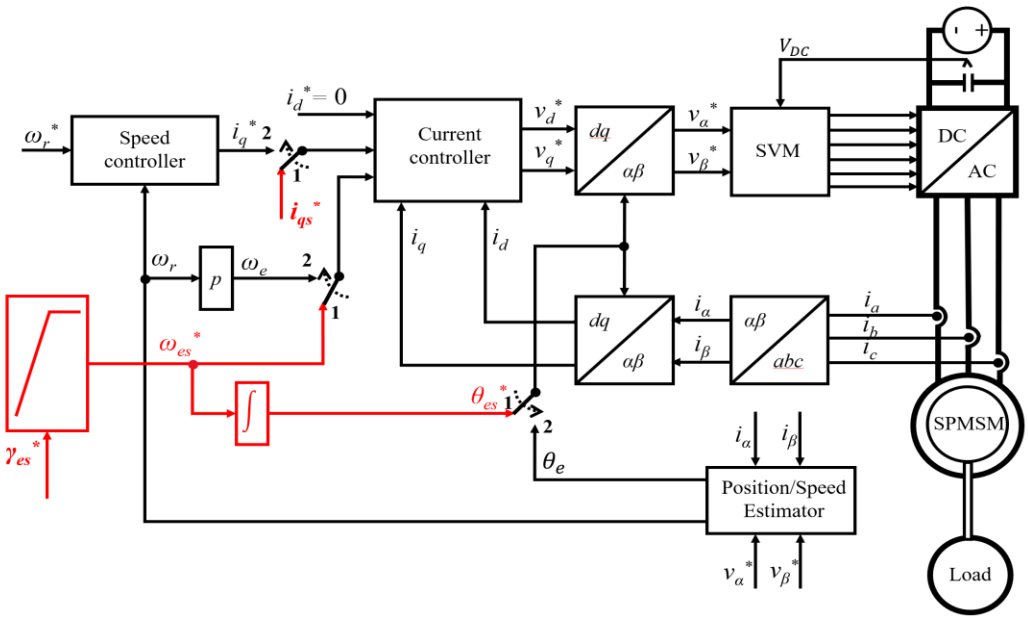


**Figure 1:** SPMSM drive control block diagram.

$$\Delta\theta_e = \theta_{es}^{*} - \theta_e \tag{10}$$

Differentiating first and second order both sides (10) yields the following equations:

$$\frac{d(\Delta\theta_e)}{dt} = \frac{d\theta_{es}^{*}}{dt} - \frac{d\theta_e}{dt} \tag{11}$$

$$\frac{d^2(\Delta\theta_e)}{dt^2} = \frac{d^2\theta_{es}^{*}}{dt^2} - \frac{d^2\theta_e}{dt^2} \tag{12}$$

Substituting (4), (7), (8), (9) into (11), (12), we can obtain:

$$\frac{d(\Delta\theta_e)}{dt} = \omega_{es}^{*} - \omega_e \tag{13}$$

$$\frac{d^2(\Delta\theta_e)}{dt^2} = \gamma_{es}^{*} - \frac{(1.5p\lambda_m i_q - T_L)p}{J_m} \tag{14}$$

Dynamical stability of the system can be achieved only if both the first and second order differentials of $\Delta\theta_e$ maintain or oscillate around zero. However, the two variables $\Delta\theta_e$ and $i_q$ change depending on each other. To show the dynamic stability condition, we first need to show the relationship between these two variables. As shown in Figure 2 along with the real and virtual rotating reference frames, the two stator current components on the real rotating reference frame are defined as follows:

$$\begin{cases} i_d = -i_{qs}^{*}\sin(\Delta\theta_e) \\ i_q = i_{qs}^{*}\cos(\Delta\theta_e) \end{cases} \tag{15}$$

Note that, since the electromagnetic torque of the PMSM depends only on $i_q$, the influence of the $i_d$ can be ignored. In Figure 2, the two cases introduce equal current $i_q$, or in other words, introduce the same electromagnetic torque. However, the influence of the virtual rotating reference frame in the case of leading or lagging has different effects on the system. It is worth mentioning that the system becomes unstable when $\cos(\Delta\theta_e)$ has a negative value, causing the two reference frames to rotate in opposite directions.

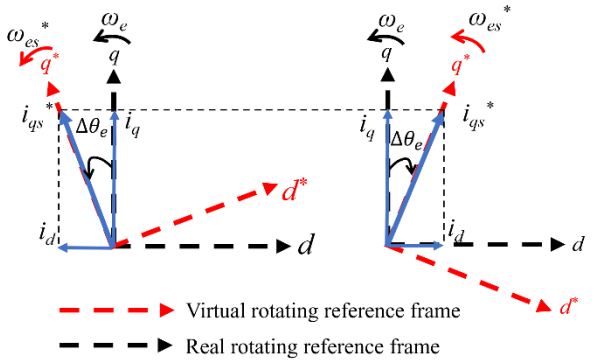


**Figure 2:** Leading virtual rotating reference frame (left) and lagging virtual rotating reference frame (right).

### 3.1.1. *Leading virtual rotating reference frame*

At the starting time of the system, both the virtual rotating reference frame and the real rotating reference frame are at zero speed. The virtual rotating reference system has a rotating speed that changes over time as (8), which takes place instantaneously. The real rotating reference frame is not only affected by the load torque and mechanical inertia but also by the response speed of the current control loop. The rotation of the real rotating reference frame does not take place immediately, and even reverses in cases of constant load torque.

The difference between the immediate rotation of the virtual rotating reference frame and the slower rotation of the real rotating reference frame gives the virtual rotating reference frame the lead. Analyzing the increase of $\Delta\theta_e$ in this case, the magnitude of real current $i_q$ decreases as the virtual rotating reference frame becomes more geometrically ahead as shown in Figure 2 (left), leading to two possible situations. The first situation, the electromagnetic process does not act in time, the virtual reference frame rotates ahead at an angle greater than $90^0$. The generated electromagnetic torque has negative value, the system falls into an unstable state due to the two reference frame will be opposite each other. The second situation, the electromagnetic process acts fast enough, the electromagnetic torque generated is large enough so that the real rotating reference frame can catch up and lead the virtual rotating reference frame. Analyzing the dynamic characteristics based on (14) and (15), the influence of the cosine component causes the motor speed response to fluctuate, then it can be stable or unstable depends on whether the initial angle error value is small or large. On the other hand, the rapid impact of the electromagnetic process creates a large electromagnetic torque forcibly and changes over time, plus the cosine component makes the amplitude of mechanical fluctuations very large. This phenomenon has negative effects if performed on practical applications, such as causing cavitation in water pumps, vibrations on lifting cranes, etc.

In summary, the case of the virtual rotating reference frame leading the real rotating reference frame has negative effects or causes instability to the system, which must be avoided.

Condition in angle difference between the virtual rotating reference frame and the real rotating reference frame at the starting time is determined as follows:

$$\Delta\theta_e(0) \le 0 \tag{16}$$

Condition (16) is not a prerequisite but is only meaningful for optimizing the system startup process. A small positive value of $\Delta\theta_e(0)$ can still make the system approach stability but the initial fluctuation is large as analyzed above. This is only the upper limit of the condition, the lower limit will be shown in the case of a lagging virtual rotating reference frame.

### 3.1.2. *Lagging virtual rotating reference frame*

Similar to the case of leading virtual rotating reference frame regarding difference between the immediate rotation of the real rotating reference frame and the slower rotation of the virtual rotating reference frame. However, the system response occurs differently in the case of a lagging virtual rotating reference frame. The rotation speed of the virtual rotating reference frame is larger than the real rotating reference system, resulting in the angle of $\Delta\theta_e$ being reduced. As depicted in Figure 2 (right) and (15), the $i_q$ value is covariated with $\Delta\theta_e$ in this case, the electromagnetic torque generated is larger, causing the real rotating reference system to accelerate further. The speed of the real rotating reference frame is greater than that of the virtual rotating reference frame then, making the

angle $\Delta\theta_e$ wider (more negative). The more negative the value of $\Delta\theta_e$ causes the electromagnetic torque to be decreased and the real rotational reference frame acceleration to be decreased. Again, the angle of $\Delta\theta_e$ is decreased. A steady state is established when the speeds and accelerations of the real rotating reference frame and the virtual rotating reference frame are equal. Compared to (13) and (14), both first and second order differentials reach zero value as pointed out before. This oscillation is "softer" than in the case of the leading virtual rotating reference frame. This phenomenon is called self-stabilizing mechanism.

However, mathematically, the self-stabilizing mechanism only occurs when the acceleration of the real rotating reference system is greater than the acceleration of the virtual rotating reference system at the initial time. This condition is given to help that the speed of the real rotating reference frame can be greater or equal to the speed of the virtual rotating reference frame and the virtual rotating reference frame is not always lead. From this analysis combining (14) and (15) we have the following condition:

$$\gamma_{es}^{*} < \frac{\left[1.5p\lambda_m i_{qs}^{*}\cos\Delta\theta_e(0) - T_L\right]p}{J_m} \tag{17}$$

Because $\gamma_{es}^{*}$ has a constant positive value, the right-hand side of (17) must also be positive, combining (16) the condition on the angle error between the virtual rotating reference frame and the real rotating reference frame at the starting time is determined as follows:

$$-\arccos\left(\frac{T_L}{1.5p\lambda_m i_{qs}^{*}}\right) \le \Delta\theta_e(0) \le 0 \tag{18}$$

It can be deduced from (17) and (18) that the electromagnetic torque generated by $i_{qs}^{*}$ not only balances the load torque but also creates acceleration for the starting process. The larger the $i_{qs}^{*}$ value is set, the more the initial angle error range that satisfies (18) is expanded, but is limited by the rated current amplitude of the motor to ensure no overcurrent occurs in the stator. The set acceleration of the virtual rotating reference frame $\gamma_{es}^{*}$ has a lower limit to ensure the startup time is quick. The smaller the value of $\gamma_{es}^{*}$, the longer the starting time. Furthermore, it increases the speed fluctuation of the transmission system. The speed fluctuation amplitude is described by the relative acceleration deviation and is defined as follows:

$$\delta_\gamma = \frac{\left[\frac{\left(1.5p\lambda_m i_{qs}^{*} - T_{L.\max}\right)p}{J_m} - \gamma_{es}^{*}\right]}{\frac{\left(1.5p\lambda_m i_{qs}^{*} - T_{L.\max}\right)p}{J_m}} \times 100\% \tag{19}$$

where $T_{L.max}$ is the largest load torque during the startup stage. The larger value of $\delta_\gamma$ can cause larger oscillation at startup. When choosing the two parameters $i_{qs}^{*}$ and $\gamma_{es}^{*}$, it is necessary to ensure that condition (17) is satisfied and make $\delta_\gamma$ as small as possible so that the initial fluctuations are small.

The acceleration characteristic as a ramp function of $\omega_{es}^{*}$ is illustrated in Figure3, $\omega_{es}^{*}$ achieves the $\omega_{es0}^{*}$ at time $t_0$ and is kept constant for a short period of time. At time $t_1$, the smooth transition algorithm begins to be executed.

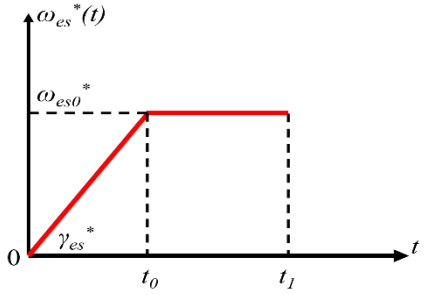


**Figure 3:** Virtual rotating reference frame acceleration with *I-f* startup.

### 3.2. Smooth transition stage

When the motor rotates at a constant speed, the electromagnetic torque is in balance with the load torque according to (6). Since the value of $i_{qs}^{*}$ is set much larger than $i_q$ so that the acceleration process is performed quickly, according to (15) there exists a non-zero $\Delta\theta_e$ after the end of the acceleration period. The conversion from *I-f mode* to *PI mode* will lead to a large peak current and torque pulse because there is a large change in the Park transformation related to the angular position. The purpose of the smooth transition phase is to get $\Delta\theta_e$ closer to zero before switching to *PI mode*.

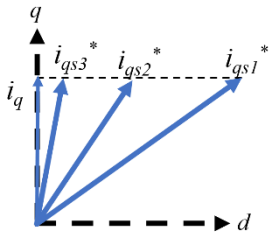


**Figure 4:** Virtual current vector moves closer to the *q* axis of the real rotating reference frame as the magnitude is reduced.

At steady state, the virtual rotating reference system always lags behind the real rotating reference system. By decreasing the set value of $i_{qs}^{*}$, $\Delta\theta_e$ can approach zero as illustrated in Figure 4. Linear method of reducing $i_{qs}^{*}$calculated according to the ramp function is performed as follows:

$$i_{qs}^{*}(t) = i_{qs1}^{*}\left(1 - \frac{t - t_1}{T_r}\right) \tag{20}$$

where $i_{qs1}^{*}$ is the current value at time $t_1$, $T_r$ is the time coefficient for reducing the current to zero.

At speed $\omega_{es0}^{*}$, the rotor angular position can already be estimated with small errors, which means that the value of $\Delta\theta_e$ can be determined. The *PI mode* is switched when the conditions (21) and (22) are satisfied.

$$\Delta\theta_e \le \varepsilon_\theta \tag{21}$$

$$i_{qs}^{*} \le \varepsilon_i \tag{22}$$

The value $\varepsilon_\theta$ is chosen depending on the error of the estimation stage and the time constant of the current control loop. Condition (22) is an additional condition in the case of light load, the current has decreased to zero but (21) has not been satisfied, the value $\varepsilon_i$ is chosen to avoid the current from continuing to decrease to negative. Finally, the integral component of the PI speed controller needs to be initialized to the appropriate value. If not initialized at the time of switching, the applied current will be suddenly reduced. The initial value of integral component is set as $i_{qs}^*(t_3)$, where $t_3$ is the time when the mode switching conditions are satisfied.

### 3.3. *I-f* starting method summary

The *I-f* startup method can be summarized as follows:
Step 1: Select parameters that satisfy conditions (17) and (18) and then start the system.
Step 2: Keep the virtual rotating reference frame rotation speed value constant for a short time when the required speed threshold is reached.
Step 3: Reduce the set current until conditions (21) or (22) are satisfied.
Step 4: Initialize the integral component of speed controller and then switch from *I-f mode* to *PI mode*.

## 4. Simulation

### 4.1. Simulation parameter

The simulation was performed on Matlab-Simulink to verify the algorithms presented in section 3. The PMSM specification are given in Table 1. Conditions to be investigated include angular acceleration conditions in section 4.2 and initial angle error in section 4.3, simulation results of smooth transition algorithm between *I-f mode* and *PI mode* are also given in section 4.4.
To have a basis for evaluating practical applicability, the mechanical characteristics of industrial fan loads are used in the simulation. This fan has the following equivalent load characteristics as follows:

$$T_L = T_{L0} + k_L \omega^2 \tag{23}$$

where, $T_{L0}$ is the initial load torque, $k_L$ is the load factor which proportional to the square of the speed. With the motor parameters in Table 1, the load characteristics are selected: $T_{L0}$ is 4.8 Nm, $k_L$ is 0.001.
For the purpose of accelerating the motor to 35% of the rated speed, the load torque at this speed is 6.1 Nm, equivalent to 38% of the motor rated torque. The current applied to the current controller must be 40% or more of the rated current, corresponding to a current $i_{qs}^*$ value of 3.5 A.

**Table 1:** PMSM specification

| SPMSM | | | |
|---|---|---|---|
| Rated power | 2 kW | Stator reistance | 0.9585 Ω |
| Rated current | 10 A | Stator inductance | 0.0053 H |
| Rated speed | 1000 rpm | Rated flux linkage | 0.1827 Wb |
| Rated DC voltage | 300 V | Moment of inertia | 0.0046 kgm$^2$ |
| Rated Torque | 16 Nm | Pole pairs | 6 |

### 4.2. Angular acceleration condition verification

In this section, conditions (17) and (19) are verified and evaluated. Three main cases can be occured when choosing the angular acceleration parameter for the virtual rotating reference frame $\gamma_{es}^*$and the applied current $i_{qs}^*$ for the system response: the acceleration process is smooth, the oscillation occurs in acceleration process, and the acceleration process becomes unstable.

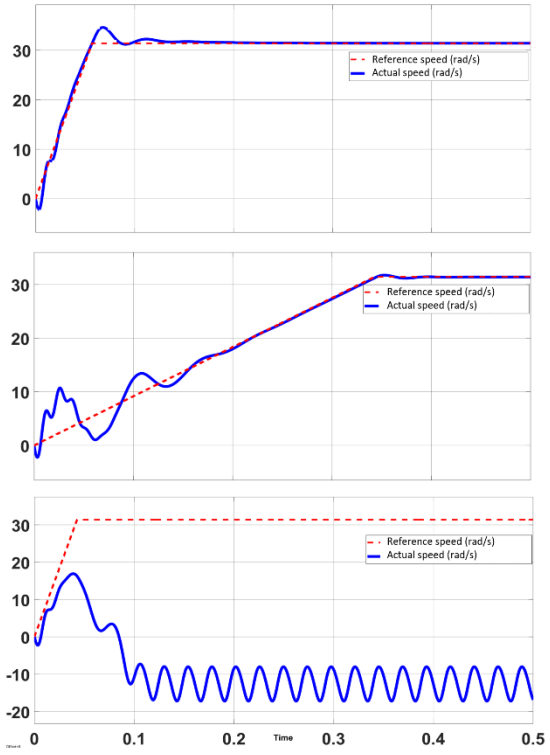


**Figure5:** Waveforms of speed $\omega_r$ (rad/s) with various values of angular acceleration: a) $\gamma_{es}^*$ = 3300 rad/s$^2$; b) $\gamma_{es}^*$ = 550 rad/s$^2$; c) $\gamma_{es}^*$ = 4400 rad/s$^2$

Choosing $i_{qs}^*$ of 4 A, set the initial angle error $\Delta\theta_e$ to $0^0$, from (17), condition $\gamma_{es}^*$ < 3368 rad/s$^2$ is obtained. The results of the motor speed response in the simulation are given in Figure 5, from top to bottom, respectively, in three cases where the set acceleration for the virtual rotating reference system has the following values: a) $\gamma_{es}$* = 3300 rad /s$^2$; b) $\gamma_{es}$* = 550 rad/s$^2$; $\gamma_{es}^*$= 4400 rad/s$^2$. The speed setting for the motor rotor is accelerated and kept constant at 35% of the rated speed, corresponding to a value of 36.65 rad/s.
In the case $\gamma_{es}^*$ = 3300 rad/s$^2$, close to the upper limit of the angular acceleration condition, the speed response almost follows the reference one. In case $\gamma_{es}^*$ = 550 rad/s$^2$, the speed response has large initial fluctuations, but then still follows the reference one. In the case $\gamma_{es}^*$ = 4400 rad/s$^2$, the acceleration process is unstable, the speed response cannot follow the reference one.

### 4.3. Initial angle error condition verification

In this case the initial position of the rotor is not known so there is an initial angle error between the virtual rotating reference frame and the real rotating reference frame that associated with the rotor flux vector. To clarify the influence in this case, the initial angle error condition (18) is included in the simulation for observation, evaluation, and verification.

It is noted from Figure 6 that $\Delta\theta_e(0) = 10^0$ corresponding to leading virtual rotating reference frame can cause the system to be unstable. In contrast, the acceleration process of virtual rotating reference frame can be stable with $\Delta\theta_e(0) = -10^0$ and $\Delta\theta_e(0) = -60^0$. However, if the requirement of $\Delta\theta_e(0)$ in (18) is not met, that acceleration process becomes unstable, e.g., $\Delta\theta_e(0) = -75^0$.

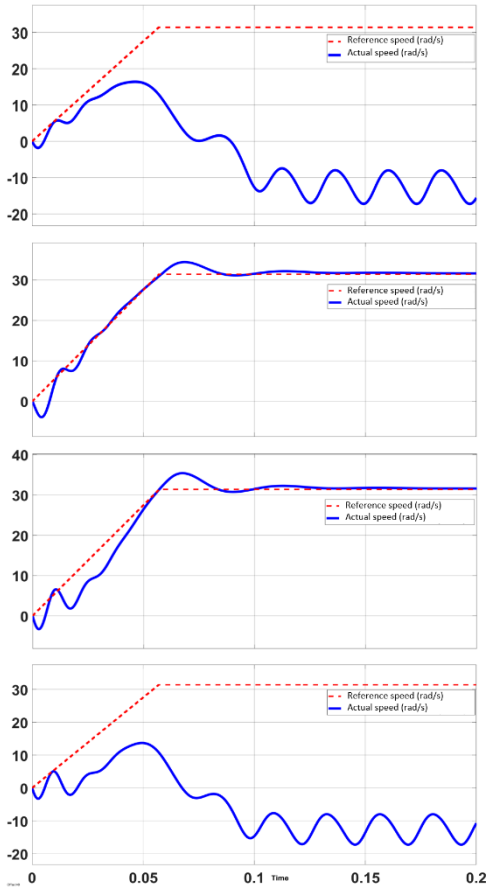


**Figure 6:** Waveforms of speed $\omega_r$ (rad/s) with various values of initial angle error: a) $\Delta\theta_e(0) = 10^0$; b) $\Delta\theta_e(0) = -10^0$; c) $\Delta\theta_e(0) = -60^0$; d) $\Delta\theta_e(0) = -75^0$

### 4.4. Smooth transition algorithm verification

The current response id and iq according to the real rotating reference frame without smooth switching algorithm is given in Figure 7. When suddenly switching from I-f mode to PI mode at t = 0.25s, the id current peaks at -17 A and the iq current peaks at 20 A. If this phenomenon occurs in the real system, the converter switches may be immediately damaged.

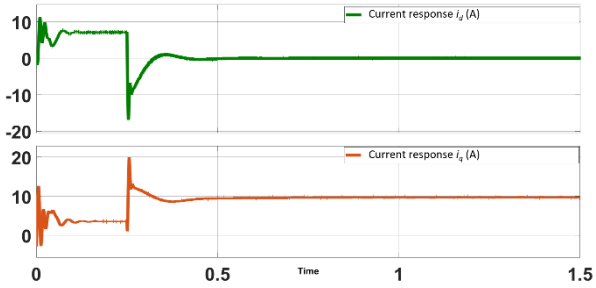


**Figure7:** Current response $i_d$ (A) and $i_q$ (A) in real rotating reference frame without smooth transition algorithm.

Figure 8 shows the current response results when the smooth transition algorithm is performed starting from $t = 0.25$ s. According to (20), the applied current $i_{qs}^*$ is reduced according to the ramp function with $T_r = 0.8$, but as shown in Figure8, the current $i_q$ does not decrease but only the current $i_d$ decreases linearly. This can be explained according to (15), $i_{qs}^*$ is decomposed into two components, the current $i_q$ to generate torque balanced with the load torque should have a constant value and only the current $i_d$ decreases. After $t = 0.7$s, when condition (21) is satisfied, *PI mode* is switched, the large peak current pulse does not appear, no overcurrent occurs.

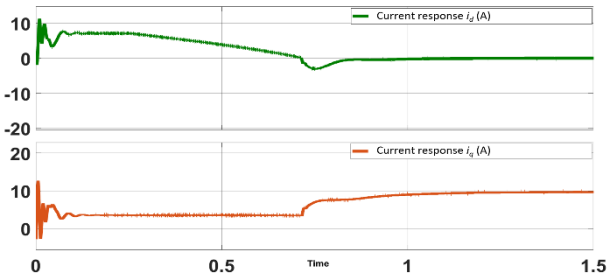


**Figure 8:** Current response $i_d$ (A) and $i_q$ (A) in real rotating reference frame with smooth transition algorithm.

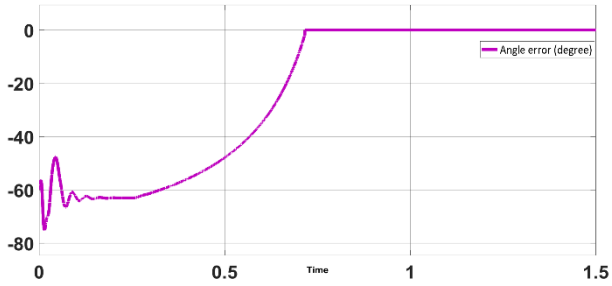


**Figure 9:** Angle error (unit $^0$) between virtual rotating reference frame and real rotating reference frame during both acceleration, smooth transition, and *PI mode*.

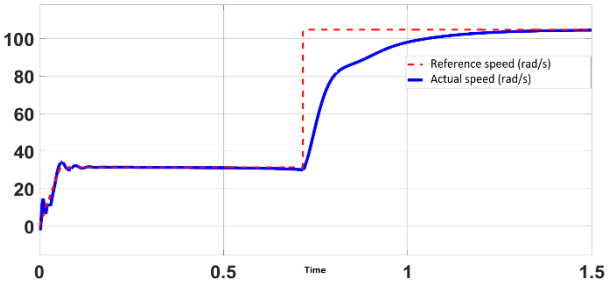


**Figure 10:** Waveform of motor speed $\omega_r$ (rad/s) in both acceleration, smooth transition and *PI mode*.

The simulation results of the angle error between the virtual and real rotating reference frames are shown in Figure 9, and waveform of the speed response is illustrated in Figure 10. During the smooth transition stage, the angle error is gradually reduced to zero, the motor rotation speed is almost constant. When switching modes, the motor speed changes smoothly.

## 5. Conclusion

The angular acceleration condition of the virtual rotating reference system has been analyzed and verified by simulation. The angular acceleration of the virtual rotating reference frame which is chosen too small will cause oscillations or if it is chosen too large, the system will become unstable. Besides, the influence of the different positions of the virtual rotating reference frame compared to the real rotating reference frame at the time of startup is also clarified. Therefore, it is necessary to ensure that virtual rotating reference frame lags the real one, and angle error between them is sufficiently small when the initial load torque is large. The PMSM drive system can reach a self-stabilizing state if the pre-specified conditions of angular acceleration of the virtual rotating reference frame and initial angle error in the acceleration stage are satisfied. The smooth transition stage is added to overcome the difficulty of peak current pusle when switching from *I-f mode* to *PI mode* caused by angle error between the two rotating reference frames. The algorithm that reduces the virtual current reference using ramp function a simple but effective, causing the phase difference between two rotating reference frames to approach zero value. The *I-f* starting method has shown its ability to overcome the difficulty of rotor position estimation at low-speed regions in theory, and it has great potential for employment in practical applications, especially low-cost applications that speed sensor is not included.

## Acknowledgement

This research is funded by Hanoi University of Science and Technology (HUST) under project number T2022-TT-012.

## References

[1] F. Yusivar, N. Hidayat, R. Gunawan, and A. Halim, "Implementation of Field Oriented Control for Permanent Magnet Synchronous Motor" *IEEE Inter. Conf. Electrical Engineering and Computer Science*, pp. 359-362, Nov. 2014.

[2] K-W. Lee, and J-I. Ha, "Evaluation of Back-EMF Estimators for Sensorless Control of Permanent Magnet Synchronous Motors", *Journal of Power Electronics*, Vol. 12, No. 4, pp. 2092-2100, July 2012.

[3] F. Genduso, R. Miceli, C. Rando, and G. R. Galluzzo, "Back EMF Sensorless-Control Algorithm for High-Dynamic Performance PMSM", *IEEE Trans. Ind. Electron.*, Vol. 57, No. 6, pp. 604-614, June 2010.

[4] Z. Q. Zhu, A. H. Almarhoon, and P. L. Xu, "Improved Rotor Position Estimation Accuracy by Rotating Carrier Signal Injection Utilizing Zero-Sequence Carrier Voltage for Dual Three-Phase PMSM", *IEEE Trans. Ind. Electron*., Vol. 64, No. 6, pp. 4452-4462, June 2017.

[5] R. Ni, K. Lu, F. Blaabjerg, and D. Xu, "A Comparative Study on Pulse Sinusoidal High Frequency Voltage Injection and INFORM Methods for PMSM Position Sensorless Control", *42nd annual Conf. IEEE Ind. Electron.*, pp. 2600-2605, Oct. 2016.

[6] S. C. Agarlita, I. Boldea, and F. Blaabjerg, "High Frequency Injection Assisted 'Active Flux' Based Sensorless Vector Control of Reluctance Synchronous Motors, With Experiments from Zero Speed", *IEEE Trans. Ind. Electron*. Vol. 48, No. 6, pp. 2725-2732, Dec. 2012.

[7] D. M. Miracle, P. D. Chandana Perera, S. Galceran-Arellano and F. Blaabjerg, "Sensorless V/f Control of Permanent Magnet Synchronous Motors", in *Motion Control*, pp. 439-458, January 2010.

[8] C. Aijun and J. Xinhai, "A Stable V/f Control Method for Permanent Magnet Synchronous Motor Drives", *IEEE Trans. Electrification Cond., Harbin, China,* Aug. 2017.

[9] I. Boldea, N. Muntean, and E. Hauler, "Distributed Anisotropy Rotor Synchronous Motors Proving High Motor Performances and New Motion Sensorless Controller", *in Record of PCIM-1992*, Vol. 2, January 1992.

[10] M. Fatu, R. Teodorescu, I. Boldea, G. D. Andreescu, and F. Blaabjerg, "I-F Starting Method with Smooth Transition to EMF Based Motion-Sensorless Vector Control of PM Synchronous Motor/Generator", *IEEE Power Electro. Specialists Conf*., pp. 1481-1487, Aug. 2008.

[11] Z. Wang, K. Lu, and F. Blaabjerg, "A Simple Startup Strategy Based on Current Regulation for Back-EMF-Based Sensorless Control of PMSM", *IEEE Trans. Power Electron.*, Vol. 27, No. 8, pp, 3817-3825, August 2012.

[12] M. Wang, Y. Xu, J. Zou, and H. Lan, (2017) "An Optimized I-F Startup Method for BEMF-based Sensorless Control of SPMSM", *IEEE Trans. Electron.*, Aug. 2017.

[13] J. Xing, Z. Qin, C. Lin, and X. Jiang, "Research on Startup Process for Sensorless Control of PMSMs Based on I-F Method Combined with an Adaptive Compensator", *IEEE Access*, Vol. 8, April 2020.

[14] D. Chen, K. Lu and D. Wang, "An I-f startup method with compensation loops for PMSM with smooth transition", *IEEJ Jour. Ind. App.* Vol. 9, No. 3, pp.263-270, Oct. 2019.

[15] D. Chen, K. Lu, and D. Wang, "An I-f Startup Method for Back-EMF based Sensorless FOC of PMSMs with Improved Stability During the Transition", *IEEE Ind. Electron. App.* Nov. 2020.

[16] W. Wang, Z. Li and X. Xu, "A Novel Smooth Transition Strategy for BEMF-Based Sensorless Drive Startup of PMSM", *Proceeding of the 11th World Cong. Intell. Ctrl. Auto.*, pp. 4296-4301, July 2014.

[17] Q. Li, X. Wang, J. Jiang, Q. Zhang, and Q. Tong, "Sensorless Control for Surface Mounted PM Machine with a High Inertial Load", *IEEE Trans. Elec. Machines and Sys.*, Vol. 2, No. 1, pp. 116-122, March 2018.

[1] W. S. Jung, H. K. Lee, Y. K. Lee, S. M. Kim, J. I. Lee, J. Y. Choi, "Analysis and Comparison of Permanent Magnet Synchronous Motors According to Rotor Type under the Same Design Specifications", *MDPI Jour. Energies*, Vol. 16, No. 3, January 2023